

Received July 20, 2018, accepted August 17, 2018, date of publication September 10, 2018, date of current version September 28, 2018.

Digital Object Identifier 10.1109/ACCESS.2018.2868448

# Radio Resource Allocation in Collaborative Cognitive Radio Networks Based on Primary Sensing Profile

DEEPAK G. C.<sup>1</sup>, (Member, IEEE), KEIVAN NAVAI<sup>2</sup>, (Senior Member, IEEE),  
AND QIANG NI<sup>2</sup>, (Senior Member, IEEE)

<sup>1</sup>MINT Lab, School of Computer Science and Mathematics, Kingston University London, Kingston KT1 2EE, U.K.

<sup>2</sup>InfoLab21, School of Computing and Communications, Lancaster University, Lancaster LA1 4YW, U.K.

Corresponding author: Deepak G. C. (d.gc@kingston.ac.uk)

This work was supported in part by the U.K. Engineering and Physical Sciences Research Council through the Project DARE under Grant EP/P028764/1 and in part by the EU Horizon 2020 Project under Grant 690750-ATOM-H2020-MSCA-RISE-2015.

**ABSTRACT** In this paper, we present a novel power allocation scheme for multicarrier cognitive radio networks. The proposed scheme performs subchannel power allocation by incorporating primary users activity in adjacent cells. Therefore, we first define the *aggregated subchannel activity index* (ASAI) as an average indicator which characterizes the collective networkwide primary users' communication activity level. The optimal transmit power allocation is then obtained with the objective of maximizing a total utility function at the secondary base station (SBS), subject to the maximum SBS transmit power, and collision probability constraint at the primary receivers. Utilizing ASAI, we further obtain an energy efficient power allocation for the secondary system. Optimal energy efficiency (EE) and spectral efficiency (SE) are contradicting objectives, and thus, there is a tradeoff between these two performance metrics. We also propose a design approach to handle this tradeoff as a function of the ASAI, which provides quantitative insights into efficient system design. In addition to a lower signaling overhead, the simulation results confirm that the proposed scheme achieves a significantly higher achievable rate. Simulation results further indicate that using ASAI enables obtaining an optimal operating point based on the tradeoff between EE and SE. The optimal operating point can be further adjusted by relaxing/restricting the sensing parameters depending on the system requirements.

**INDEX TERMS** Cognitive radio networks, energy efficiency, spectral efficiency, spectrum sensing, spectrum sharing.

## I. INTRODUCTION

In cognitive radio networks (CRN), secondary users (SUs) may opportunistically access the available spectrum during the times/in the locations, where the primary users (PUs) are not active. However, the SUs have to terminate transmission immediately if a PU starts its communications activity again. CRN is one of the envisaged solutions for improving spectral efficiency (SE), which is defined as the total capacity normalized by the available bandwidth measured in bps/Hz, in the cellular band, see [1], [2]. The main challenge in spectrum sharing is to efficiently exploit the underutilized portions of the spectrum without compromising the quality-of-service (QoS) in the primary system.

The amount of the underutilized spectrum available to the CRN depends on the nature of primary users'

communication activity. Availability of the spectrum is primarily detected through robust spectrum sensing methods such as those proposed in [3]. Several spectrum sharing methods have been also proposed for the CRNs including overlay and underlay spectrum access [4]. In the overlay spectrum sharing, the secondary system accesses the channel only if the channel is idle. In the underlay method, the secondary system simultaneously utilizes the channel subject to keeping the aggregated interference at the primary receiver below a predefined threshold. This threshold is a system parameter which depends on the primary system characteristics [5]. Ideally, to assure the QoS in the primary system, in overlay (underlay) access, accurate information of spectrum sensing (i.e., perfect channel state information for the channel between the secondary transmitters and the

primary receivers) is a prerequisite. In practice however, attaining such information is challenged by no or very limited resources for inter-system signaling.

In a multicell CRN, coordination among the neighboring secondary base stations (SBS) plays a paramount role in efficient design of resource allocation [6]. Networkwide resource allocation significantly reduces the impact of intra-system interference on the overall secondary system performance. This further enables the secondary system to exploit the temporal variations of spectrum availability due to the time-varying primary system communication activity. Exploiting stochastic dynamics of the available spectrum enhances the performance of the radio resource allocation in the secondary system [7].

Several schemes have been proposed which are designed to exploit the primary service activity, however it is usually assumed that the activity information is available to the secondary system, either through signaling or a priori knowledge, see [5]. Yet, this assumption may not always be valid in practical scenarios where multicell networks are considered. Our previous work [8] has partially dealt with this issue by proposing a collaborative approach among SBSs to estimate the primary system communication activity on the subchannels to maximize the SE. In this paper, we incorporate the primary subchannels activity into transmission power allocation at the SBS, such that the maximum possible SE is achieved. The proposed method simplifies the power allocation method in CRN while significantly reducing the corresponding signaling overhead.

We also investigate the impact of the proposed primary channel activity profile on the energy efficiency (EE) of the system. Here, EE measures how efficiently the available energy is utilized to maintain the QoS in the end-to-end communications [9]. The EE metric can be defined in various forms such as energy-per-bit to noise power spectral density ratio, i.e.,  $E_b/N_0$ , bit per Joule capacity, rate per energy, or Joule per bit, however they are essentially equivalent and mutually convertible [10]. For EE resource allocation, an energy-per-goodbit metric is considered in [11] that adopts the spectrum sharing along with soft-sensing information by adaptively setting the sensing threshold. Energy and spectral efficient design for CRN is also studied in [12] and [13] to optimize one of them during a frame duration.

Accuracy of the spectrum status estimation directly affects the achieved EE, however such information might not be available to the SU transmitter [14]. To tackle this issue, instead of using perfect subchannel availability status, our proposed method utilizes the estimated primary users' activity on each subchannel. Primary users' activity is estimated using a simple method with very low signaling overhead.

The primary system communication activity on a subchannel is a function of PUs' arrival and departure rates and thus has a random nature. To characterize this, here we define a new parameter, *subchannel activity index* (SAI), which

indicates the level of communication activity in a primary subchannels. Therefore, SAI is a probabilistic metric which is based on the limited number of sensing results. In this paper, we then propose schemes to evaluate the *aggregated SAI* (ASAI). The ASAI is then utilized in an optimal power allocation design in the secondary system to manage the tradeoff between the SE and EE.

A low SAI indicates an underutilized subchannel which may accommodate SUs. This is however subject to careful and controlled power allocation to avoid compromising primary system's communication quality. In a secondary cell, ASAI for a subchannel indicates the activity of the PUs located in that particular cell, as well as the PUs accessing the same subchannels in the adjacent cells. To estimate ASAI, we then propose a simple, yet efficient, collaborative spectrum monitoring scheme with very low signaling overhead. In the proposed scheme, the required information is one bit per subchannel feedback transmitted by adjacent SBSs.

In cases where the SBS allocates a higher transmission power to the subchannels with a higher ASAI, the minimum QoS requirements for the primary services might be compromised along with significant degradation on EE. In the secondary system however, a more conservative power allocation to a subchannel with a lower ASAI may result in a lower SE. To model this tradeoff, we adopt the notion of utility function [15], [16]. To characterize SE (EE), a utility function is defined for each subchannel which is an increasing function of the achievable rate (achievable rate normalized by the corresponding allocated power). Both utility functions are also a decreasing function of the ASAI.

Optimal power allocation method is then formulated in which the objective is to maximize the total SBS utility, in terms of the SE, subject to total available transmit power at the SBS and primary system collision probability constraints. For the same system settings, we also formulate the optimal power allocation with the objective of maximizing total SBS utility, in terms of EE, subject to the similar constraints described above. The formulated problems are the instances of weighted sum-rate maximization which have been widely studied in the related literature, see [6], [17], [18]. Most of the previous works are based upon accurate channel state information and/or spectrum sensing, thus need direct inter-system and heavy intra-system signaling. Our proposed method does not require inter-system signaling, and the signaling overhead in the secondary system is very low as it needs only one bit per subchannel.

The contributions of this paper are as follows:

- We propose and characterize the SAI as an indicator of activities level of the PUs in their corresponding subchannels. We then propose a simple yet efficient collaborative spectrum monitoring among the base stations with very low signaling overhead to obtain the *aggregated SAI* (ASAI).
- A utility function is then defined to incorporate the ASAI into the corresponding spectral efficiency for all subchannels. We then formulate the joint efficient transmit

power and subchannel allocation schemes in the SBS to maximize the total SBS utility function.

- We further applied ASAI to achieve the energy efficient resource allocation technique. Similar to the previous case, we define a utility function to characterize energy efficiency. Energy efficient power allocation is then obtained by maximizing the total system utility. The obtained solutions can also be extended to other scenarios.
- We then study the system performance in terms of EE and SE against reference system models. Simulation results show that the proposed method closely follows the ideal spectrum access with a slightly lower achievable rate, whereas the required signaling overhead is significantly reduced. The results further indicate that using ASAI enables obtaining an optimal operating point based on the tradeoff between EE and SE. The optimal operating point can be further adjusted by relaxing/restricting the sensing parameters depending on the system requirements. Such a EE and SE tradeoff management has never been studied before in the literature. The obtained EE and SE relation based on ASAI in the proposed method is practically more efficient than the conventional EE and SE tradeoff which is, in most cases, based on the transmit power.

The rest of this paper is organized as follows. Section II presents the system model and defines the notion of ASAI. Section III presents the problem formulation and maximizing system utility. In Section IV, energy efficient power allocation is presented. Section V includes the simulation results followed by conclusions in Section VI.

## II. SYSTEM MODEL

### A. CHANNEL MODEL

The considered system includes a cellular CRN, also referred to as the secondary system, co-located with legacy primary system. The primary network could be cellular network or TV broadcaster, whereas the secondary network could possibly be femtocell, tactical network or even a heterogeneous network. Here, we consider a primary base station which serves a number of PUs within the transmission range. In such cases, the available subchannels vary over space and time which makes it difficult to achieve reliable spectrum allocation. However, the analysis and simulation results in this paper are equally valid for different primary networks.

A schematic of the considered network is presented in Fig. 1. A  $B$  Hz frequency band is licensed to the primary system which serves PUs indexed by  $j \in \{1, \dots, J\}$ . The spectrum of the primary system is shared with secondary system for downlink transmission. The CRN is a multicell network with  $M$  secondary base stations (SBSs). In the central cell, SBS serves SUs indexed by  $s \in \{1, \dots, S\}$ . The secondary system utilizes orthogonal frequency division multiple access (OFDMA), where the radio spectrum is divided into  $N$  non-overlapping  $B_i = B/N$  Hz subchannels which are indexed by  $i \in \{1, \dots, N\}$ . The considered network

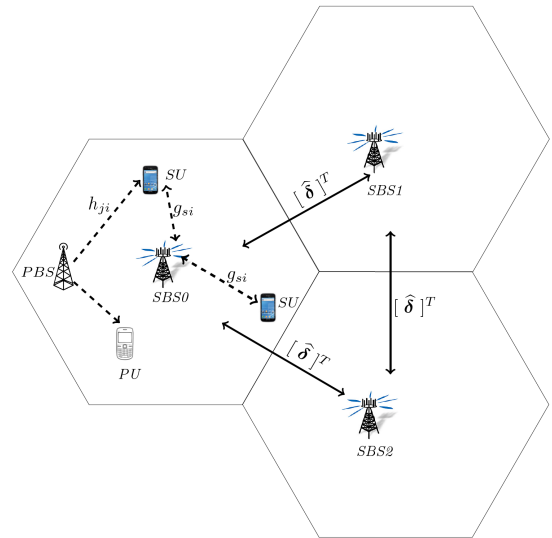


FIGURE 1. A schematic of the considered cognitive cellular network.

scenario and proposed resource allocation method are equally applicable for uplink transmission by considering appropriate access scheme, e.g., single carrier FDMA (SC-FDMA), to improve the power efficiency of user devices. Moreover, the user terminals should be able to estimate uplink channel state information.

The communication link between the secondary transmitter to the secondary receivers and secondary transmitter to the primary receivers, for subchannel  $i \in \{1, \dots, N\}$ , are referred to as secondary channel, and interference channel, which are denoted by  $g_{si}(v)$ , and  $h_{ji}(v)$ , respectively. Parameter  $v$  denotes the joint fading state which is dropped hereafter for brevity. The value of  $g_{si}$  is updated through the measurement in each time frame by the CRN user. Making  $h_{ji}$  available at the secondary system is a challenging task because there is often no direct signaling between primary and secondary systems. However, similar to [19], we assume that it is estimated through the aggregated interference received at the SUs due to the primary transmission.

In this setting, the spectral efficiency for SU,  $s$ , accessing subchannel  $i$  is:

$$r_{si} = \log_2 \left( 1 + \frac{g_{si}P_{si}}{h_{ji}P_{pi} + N_0} \right) \text{ bps/Hz}, \quad (1)$$

where,  $P_{si}$  is the allocated transmission power on subchannel  $i$  at the SBS corresponding to secondary user  $s$ , therefore  $g_{si}P_{si}$  is a random variable. Furthermore,  $h_{ji}P_{pi}$  is the received interference at the secondary system due to subchannel reclaimed by the primary users which is measured at the secondary receiver and  $N_0$  is the white Gaussian noise power. We also define  $\mathbf{r}_s = [r_{s1} \dots r_{si} \dots r_{sN}]^T$  as the rate vector for secondary user  $s$ , where  $(\cdot)^T$  indicates a vector transpose operator. The optimal transmit power vector in the central SBS,  $\mathbf{P}_i^* = [P_{1i}^* \dots P_{s,i}^* \dots P_{Si}^*]^T$ , is directly related to the primary network communication activity on subchannel  $i$  as well as the associated constraints for protecting PU's QoS.

Time is slotted into frames and SBSs are synchronized in the frame level. All transmitters and receivers in the system have single antenna unless otherwise stated. There is no direct signaling between the primary and secondary systems. The secondary service either adopts underlay or overlay spectrum access technique based on each subchannel status. In underlay access, the secondary service can always access to the subchannel subject to the interference constraint for the primary system. In overlay access, the secondary service senses the subchannel status and conducts transmission if the corresponding frequency band is idle. While implementing OFDMA in CRN, the inter-channel interference is negligible due to high spectral distance and sharp bandpass filter in the secondary system [5].

**B. SPECTRUM SENSING**

We consider an energy detector spectrum sensing technique where sensing is performed in each sensing slot at the secondary terminals to determine whether the subchannel is idle or busy. Therefore, when the subchannel status is estimated, it is either a correct estimation or a sensing error. We further assume that subchannel  $i$ 's status remains unchanged during a sensing slot,  $T_i$ . The actual state of the subchannel  $i \in \{1, \dots, N\}$  is represented by hypothesis  $\{H_0, H_1\}$ , where  $H_0$  ( $H_1$ ) indicates the idle (busy) state of the subchannel. Probabilities of  $H_0$ , and  $H_1$  are denoted by  $\Pr(H_0)$ , and  $\Pr(H_1)$ , respectively.

The exact pattern of  $\Pr(H_0)$  and  $\Pr(H_1)$  can be obtained by observing the current sensing results and the previous access patterns, or by querying the available radio environment map. However, they can be analytically obtained with the help of an appropriate distribution function. It is generally the case that the subchannels are randomly accessed by PUs which approximately follow the uniform distribution over unbiased subchannel space  $\{1, \dots, N\}$ . In such a case, both probabilities are equally likely which results equi-probable hypotheses.

Here,  $\Pr(H_0)$  and  $\Pr(H_1)$  are also the indicators of channel holding time by primary system. For any arbitrary channel  $i$ , when  $\Pr(H_1)$  is higher, the duration of channel holding by PU is expected to be higher. Moreover, when a large number of subchannels are considered, the channel holding time becomes very small duration [20]. One way is to use the known distribution function as in cellular communication case, however, in cases of cognitive radio, it is estimated by using a cost effective sensing techniques or by maintaining a subchannel database.

In energy detection method, the SUs receive  $T_i f_0$  baseband complex samples during the sensing slot,  $T_i$ , where the sampling rate is  $f_0$ . Let  $Y_k$  denote the received  $k^{th}$  signal sample from PU,

$$Y_k = \begin{cases} Z_k, & : H_0, \\ X_k + Z_k, & : H_1, \end{cases} \quad (2)$$

where  $X_k$  is the received signal from PUs and  $Z_k$  is the additive white Gaussian noise (AWGN) with

variance  $\sigma_w^2 = E[|Z_k|^2]$ . The test statistic of the received signal is thus obtained as

$$E_Y = \frac{1}{T_i f_0} \sum_{k=1}^{T_i f_0} |Y_k|^2. \quad (3)$$

For each subchannel  $i$ , the test statistic is then compared with the threshold energy level,  $\epsilon_i$ , to locally obtain the status of subchannel  $i$ . In practice,  $\epsilon_i$  is a system parameter which mainly depends on the primary system requirements [18].

**C. SUBCHANNEL ACTIVITY INDEX**

For a subchannel  $i \in \{1, \dots, N\}$ , the outcomes of detection are: idle ( $E_Y < \epsilon_i | H_0$ ), busy ( $E_Y \geq \epsilon_i | H_1$ ), miss detection ( $E_Y < \epsilon_i | H_1$ ), and false alarm ( $E_Y \geq \epsilon_i | H_0$ ). In cases of any spectrum sensing methods under consideration, the error terms can never be completely avoided. In the considered energy detection method, the sensing errors, i.e., miss detection and false alarm, should be taken into consideration to model the practical cases of resource allocation in CRN. Therefore, to achieve an optimal SE and EE balance, SUs access the subchannel  $i$  when  $\Pr(idle)\Pr(H_0) + \Pr(miss\ detection)\Pr(H_1) > \Pr(busy)\Pr(H_1) + \Pr(false\ alarm)\Pr(H_0)$ . Note that the primary channel protection and spectrum utilization are defined according to the available CRN standard, i.e., IEEE 802.22 [21], as  $\Pr(detection) \geq 0.9$ , and  $\Pr(false\ alarm) \leq 0.1$ , respectively. The above condition thus reduced to the following probability ratio.

$$\Psi_i \triangleq \frac{\Pr(E_Y < \epsilon_i | H_0)\Pr(H_0) + \Pr(E_Y < \epsilon_i | H_1)\Pr(H_1)}{\Pr(E_Y \geq \epsilon_i | H_1)\Pr(H_1) + \Pr(E_Y \geq \epsilon_i | H_0)\Pr(H_0)} > 1. \quad (4)$$

*Definition 1:* We define, SAI, i.e.,  $\delta_i$ , as a measure of the primary system activity as following. (5), as shown at the bottom of the next page, where,  $\mathbb{R}\{0, 1\}$  returns a binary value with equal probability of 0 and 1.

Here, all possible sensing errors, i.e., miss detection and false alarm, have been considered in the parameter  $\delta_i$ . In cases  $\delta_i \triangleq 0$ , the activity of primary system on subchannel  $i$  is most likely minimum. In such cases, the SUs can access subchannel  $i$  with a low risk of interference. Conversely, when  $\delta_i \triangleq 1$ , it is likely that the subchannel is in use by the primary system, and thus SUs are not allowed to access the subchannel without proper transmit power control mechanism.

When the probability ratio,  $\Psi_i$  in (4) is equal to 1, although it occurs with a very low probability,  $\delta_i$  randomly selects either 0 or 1, which is basically a decision deadlock situation. If this decision does not fall towards the correct state of the subchannel, the interference to the primary transmission system is likely to be unavoidable. This situation occurs if and only if  $\Psi_i = 1$ .

In the following, we investigate the cases  $\delta_i = 0$  and  $\delta_i = 1$ , due to the fact that  $\Psi_i = 1$  is a less likely event in the considered subchannel sensing method. It is straightforward to express  $\Psi_i$  in terms of miss detection and

false alarm for the outcomes of subchannel detection method as  $\Psi_i = \frac{(1-\mathcal{P}_{fa,i})\Pr(H_0)+\mathcal{P}_{md,i}\Pr(H_1)}{(1-\mathcal{P}_{md,i})\Pr(H_1)+\mathcal{P}_{fa,i}\Pr(H_1)}$ , where for subchannel  $i \in \{1, \dots, N\}$ ,  $\mathcal{P}_{md,i}$  and  $\mathcal{P}_{fa,i}$  are the probabilities of miss detection and false alarm, respectively. The probability of detection,  $\mathcal{P}_{d,i}$ , is defined as  $1 - \mathcal{P}_{md,i}$ . Note that  $\Psi_i \in [0, +\infty)$  because  $1 + \mathcal{P}_{md,i} \geq \mathcal{P}_{fa,i}$  and  $1 + \mathcal{P}_{fa,i} \geq \mathcal{P}_{md,i}$ .

Here,  $Q\left(\left(\frac{\varepsilon_i}{\sigma_w^2} - \gamma_i - 1\right)\sqrt{\frac{T_i f_0}{2\gamma_i + 1}}\right)$  is the probability of detection,  $\mathcal{P}_{d,i}$ , for the sensing duration,  $T_i$ , and sampling frequency,  $f_0$ , where  $Q(z) := (1/\sqrt{2\pi}) \int_z^{+\infty} e^{-\tau^2/2} d\tau$ , and  $\varepsilon_i$ ,  $\sigma_w^2$ , and  $\gamma_i$  are energy detection threshold, variance of the additive white Gaussian noise at the spectrum sensors, and the average received signal to noise ratio (SNR) of primary system signal received at the spectrum sensors, respectively [22]. Similarly, the probability of false alarm,  $\mathcal{P}_{fa,i}$ , is expressed as  $Q\left(\left(\frac{\varepsilon_i}{\sigma_w^2} - 1\right)\sqrt{\frac{T_i f_0}{2\gamma_i + 1}}\right)$ . The sensing parameters are assumed to be fixed during the sensing duration.

*Theorem 1: An equiprobable subchannel  $i$  is available if*

$$\gamma_i \geq \Theta_{1i} + \Theta_{2i} \pm \Theta_{2i} \sqrt{\Theta_{2i}^2 + 2\Theta_{1i} + 1}, \quad \forall i, \quad (6)$$

where  $\gamma_i$  is the received SNR,  $\Theta_{1i} = \frac{\varepsilon_i}{\sigma_w^2} - 1$ ,  $\Theta_{2i} = \frac{Q^{-1}(1-\bar{\mathcal{P}}_{fa,i})}{\sqrt{T_i f_0}}$ ,  $\bar{\mathcal{P}}_{fa,i}$  is the false alarm probability threshold, and  $\varepsilon_i$  is the energy detection threshold.

*Proof:* See Appendix A. ■

*Remark 1: The spectrum sensing decision deadlock situation occurs when  $\Psi_i = 1$ , and thus  $\mathcal{P}_{md,i} = \mathcal{P}_{fa,i}, \forall i$ . For a given energy detector, such cases however are unlikely to occur. This can also be concluded from the complementary receiver operating characteristic (CROC) curve, i.e., plot of  $\mathcal{P}_{md,i}$  against  $\mathcal{P}_{fa,i}$ .*

When maximum tolerable false alarm probability, which is a system defined parameter, is set to  $\bar{\mathcal{P}}_{fa}$ , the corresponding decision threshold  $\frac{\varepsilon_i}{\sigma_w^2}$  is obtained. However, in the proposed method as described in Theorem 1, the parameter  $\delta_i$  determines the availability of subchannels which considers all the possible sensing errors. In such cases, the level of received SNR at the distributed sensors would be able to precisely calculate the subchannels activities. Therefore, using (6), we obtain the corresponding received SNR,  $\bar{\gamma}_i$ , as a decision variable depending on  $\bar{\mathcal{P}}_{fa}$ . In Fig. 2, the threshold  $\bar{\mathcal{P}}_{fa,i}$  versus the received SNR from primary transmitter is shown which is based on  $\delta_i$  to assist the subchannel decision process.

The SNR is obtained at  $\gamma_i = \bar{\gamma}_i$ , where  $\delta_i$  is randomly chosen, thereby introducing the interference due to imperfect decision. Here,  $\bar{\gamma}_i$  is in fact the SNR threshold based on which the subchannel availability is detected. Furthermore, when

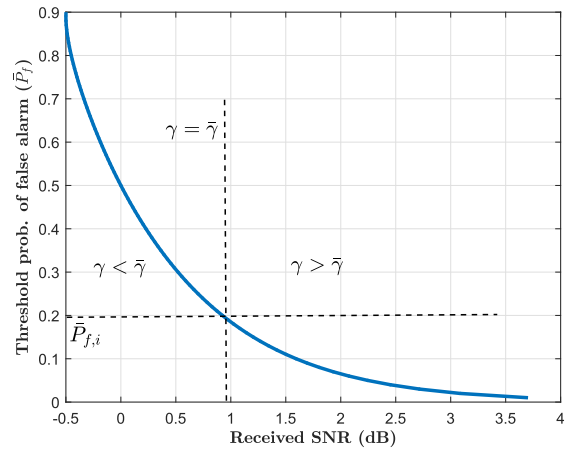


**FIGURE 2. Probability of false alarm threshold vs. the received SNR to estimate the idle (or busy) primary channels based on  $\delta_i$ .**

the condition  $\gamma_i > \bar{\gamma}_i$  ( $\gamma_i < \bar{\gamma}_i$ ) is satisfied, the interference to the primary system due to the imperfect decision is very low. The plot in Fig. 2 is presented in which all other sensing parameters including the sensing signaling overhead, frame duration, etc. are kept constant.

In cases where a lower  $\bar{\mathcal{P}}_{fa,i}$  is set, which ultimately enhances the spectrum utilization, the subchannel is available only a high received SNR regime. However when the constraint is relaxed, the condition  $\gamma_i > \bar{\gamma}_i$  is held even for lower SNR. Therefore, more subchannels become available to be accessed by the SUs. Note that in Fig. 2,  $\mathcal{P}_{md,i} = \mathcal{P}_{fa,i}$ , or  $\gamma = \bar{\gamma}$ , is the region in CROC curve around which the maximum interference occurs because of the uncertainty in decision made on the availability of subchannel  $i$ . In the considered system, having  $\gamma_i = \bar{\gamma}_i$  is however always less likely than  $\gamma_i \geq \bar{\gamma}_i$ . Therefore in the proposed method, the interference due to the random subchannel decision is negligible.

### III. INTER-CELL COLLABORATIVE SPECTRUM MONITORING

The spectrum sensing task is executed at SUs and the sensing outcomes must be transmitted to SBS where they are processed to cooperatively accumulate and estimate the status of the subchannels. Corresponding to subchannel  $i$  in SBS  $m$ , where  $m = 1, \dots, M$ , spectrum sensing returns a decision variable  $\delta_{m,i}$ . If subchannel  $i$  is busy (idle), then  $\delta_{m,i} = 1$  ( $\delta_{m,i} = 0$ ). Sensing vector,  $\delta_m = [\delta_{m,1}, \dots, \delta_{m,N}]^T$ , indicates the status of the subchannels in SBS  $m$ .

$$\delta_i \triangleq \begin{cases} 1, & \text{if } \frac{\Pr(E_y < \varepsilon_i|H_0) \Pr(H_0) + \Pr(E_y < \varepsilon_i|H_1) \Pr(H_1)}{\Pr(E_y \geq \varepsilon_i|H_1) \Pr(H_1) + \Pr(E_y \geq \varepsilon_i|H_0) \Pr(H_0)} < 1, \\ 0, & \text{if } \frac{\Pr(E_y < \varepsilon_i|H_0) \Pr(H_0) + \Pr(E_y < \varepsilon_i|H_1) \Pr(H_1)}{\Pr(E_y \geq \varepsilon_i|H_1) \Pr(H_1) + \Pr(E_y \geq \varepsilon_i|H_0) \Pr(H_0)} > 1, \\ \mathbb{R}\{0, 1\} & \text{otherwise,} \end{cases} \quad (5)$$

The cooperative detection technique of  $\delta_{m,i} \{m=1 \dots M, i \in \{1 \dots N\}\}$  is then implemented among the SBSs to obtain the *aggregated SAI* (ASAI). The subchannel sensing however is not perfect, which results the subchannel status, e.g., idle or busy, is likely subject to sensing errors.

For subchannel  $i$  in a SBS with  $M - 1$  neighboring SBSs, the ASAI is obtained as:

$$\hat{\delta}_i = \frac{1}{M} \sum_{m=1}^M w_m \delta_{m,i}, \quad \forall i, \quad (7)$$

where  $w_m$  is the weight associated with  $\delta_{m,i}$  provided by SBS  $m = 1, \dots, M$ . The value of  $w_m$  primarily depends on the priority given to the decision, e.g., depending on the distance of the neighbor SBSs. It is assumed that SBSs maintain perfect synchronization through a beacon signal such that each BS executes correct SAI information. Here, we simply consider unit weights,  $w_m = 1, \forall m$ . The weights could be also assigned based on the level of interference from the neighboring SBSs, or depending on the nature of traffic in the neighbor base stations. The aggregated activity index vector for an SBS is defined as:

$$\hat{\delta} = [\hat{\delta}_1, \dots, \hat{\delta}_N]^T, \quad (8)$$

where according to (7),  $0 \leq \hat{\delta}_i \leq 1, \forall i$ .

To obtain ASAI, each SBS only needs to transmit 1-bit information per subchannel to the neighboring SBSs. In our proposed method, each SBS broadcasts its corresponding  $\delta_i$  at the beginning of each time frame which is received and recognized by all its neighboring SBSs. Therefore, in a SBS with  $M - 1$  neighboring cells, obtaining ASAI for all  $N$  subchannels only requires  $(M - 1) \times N$  bits of feedback.

### A. COLLABORATIVE SPECTRUM ACCESS

In a given SBS, the availability of subchannel  $i$  is evaluated based on  $\hat{\delta}_i$ . The SBS then adopts an appropriate access technique for each subchannel based on its corresponding ASAI.

In this section, we propose a power allocation scheme in which incorporating  $\hat{\delta}_i$ , the transmit power of the SBS is obtained to maximize the achievable rate of the secondary system. The constraints include the maximum SBS transmit power, and the minimum QoS on the primary network. The proposed spectrum access method at the SBS based on ASAI is summarized in Algorithm 1.

There are three possible cases: *i*)  $\hat{\delta}_i = 0$ , *ii*)  $\hat{\delta}_i = 1$ , and *iii*)  $0 < \hat{\delta}_i < 1$ . For  $\hat{\delta}_i = 0$ , there is no PU transmission detected on subchannel  $i$  both within the SBS and in the neighboring cells. Therefore, overlay subchannel access is adopted for transmission over subchannel  $i$ . In cases where  $\hat{\delta}_i = 1$ , subchannel  $i$  is busy both in the SBS and its neighboring cells, therefore secondary transmission on this subchannel is not allowed. In cases where  $0 < \hat{\delta}_i < 1$  which is most likely to occur, underlay access technique is adopted by the secondary system. The larger the  $\hat{\delta}_i$ , the higher will be the chance of imposing interference on subchannel  $i$ , thus

### Algorithm 1 Inter-Cell Collaborative Spectrum Monitoring Scheme at SBS0

- 1: Neighbor SBSs, feedback  $\delta_m = [\delta_{m1}, \dots, \delta_{mN}]^T$ , to SBS0,
- 2: **for** each subchannel  $i$ , **do**
- 3:   SBS0, obtains  $\hat{\delta}_i$ , using (7)
- 4:   **if**  $\hat{\delta}_i = 1$ , **then**
- 5:     the subchannel is not allocated in SBS0.
- 6:   **else if**  $\hat{\delta}_i = 0$ , **then**
- 7:     overlay access is adopted by the SBS0 on subchannel  $i$ ,
- 8:     obtain optimal transmit power,  $\mathbf{P}_a^*$ , and maximize spectral efficiency,
- 9:     go to step (12),
- 10:   **else if**  $0 < \hat{\delta}_i < 1$ , **then**
- 11:     SBS0 adopts underlay access on subchannel  $i$  and allocates power based on scheme in Section III.D.
- 12:     obtain optimal transmit power,  $\mathbf{P}_b^*$ , based on the scheme in Section IV.
- 13:   **end if**
- 14: **end for**

the transmit power at the SBS should be adjusted accordingly to protect the subchannels used by primary system. In the following, we present subchannel power allocation, where  $0 < \hat{\delta}_i < 1$ .

### B. OPTIMAL TRANSMIT POWER ALLOCATION

Here, we propose an analytical framework for optimal subchannel power allocation based on  $\hat{\delta}_i$ , i.e.,  $0 < \hat{\delta}_i < 1$ . As it is seen in (1), the achievable rate for user  $s$  on subchannel  $i$ ,  $r_{si}$  depends on signal to noise and interference ratio, i.e.,  $g_{si}/(I_{pi} + N_0)$ , where  $I_{pi} = h_{ji}P_{pi}$  is the aggregated interference due to simultaneous transmissions by the PUs. It is assumed that the primary transmitters follow a non-adaptive and constant transmission power. On the other hand, the higher the value of  $\hat{\delta}_i$ , the higher is the activity of the primary system over subchannel  $i$ . Therefore, a higher  $P_{si}$  is required to keep  $r_{si}$  at the same level.

As the matter of fact, two subchannels  $i$  and  $k$ , having similar path loss and channel gains  $h_{ji}$  and  $h_{jk}$ , respectively, provide the same achievable rate,  $r_{si} = r_{sk}$ . Therefore,  $\hat{\delta}_i < \hat{\delta}_k$  apparently results  $I_{pi} < I_{pk}$ . Furthermore, according to (1), a higher transmit power is required to provide the same rate, i.e.,  $P_{si} < P_{sk}$ . In other words, the ‘‘cost’’ of providing the same rate to user  $s$  on subchannels  $i$  is lower than that of subchannel  $k$ .

Here, our aim is to quantify the impact of  $\hat{\delta}_i$  on the system performance at the SBS when deciding for the access method, and the transmit power on subchannel  $i$ , i.e.,  $P_{si}$ . Thus corresponding to SU  $s$ , transmitting on subchannel  $i$ , we define utility function  $u_{si}$ , measured in b/s/Hz:

$$u_{si} \triangleq \frac{r_{si}}{\hat{\delta}_i} \alpha_{si}, \quad (9)$$

where  $\alpha_{si}$  is a weight parameter which characterizes the priority level for user  $s$ , which are specified in the medium access control layer to achieve, e.g., a certain level of fairness and/or traffic load control. Here, the utility function,  $u_{si}$ , is constructed as a decreasing function of ASAI to indicate the fact that higher activities of PUs deteriorates the cognitive radio system performance in terms of spectral efficiency. Therefore, the larger the value of  $u_{si}$ , the lower is the cost of transmission on subchannel  $i$ . Total secondary system utility,  $U_a$ , is then defined as

$$U_a = \sum_{s=1}^S \sum_{i=1}^N u_{si}. \quad (10)$$

If  $0 < \hat{\delta}_i < 1$ , the SBS adopts the underlay spectrum access. Thus the interference is induced at the primary receivers. Transmission collision may then occur at the primary receiver if the inflicted interference by the secondary transmission,  $I_{ji} = \sum_{s=1}^S P_{si} h_{ji}$ ,  $\forall i, j$ , is getting higher than a predefined threshold,  $\beta_{ji}$ ,  $\forall i, j$ . To protect the QoS in the primary system, a radio resource allocation is devised so that the probability of collision in the primary system due to the simultaneous transmission by SU is kept below a threshold,  $\eta_{ji}$ , which is a primary system parameter related to the primary QoS [19]. The optimal radio resource allocation is then formulated as:

$$\mathcal{A}_1 : \max_{\mathbf{P}} U_a, \quad (11a)$$

$$\text{s.t.} \sum_{s=1}^S \sum_{i=1}^N P_{si} \leq P_T, \quad (11b)$$

$$\Pr \left\{ \sum_{s=1}^S P_{si} h_{ji} > \beta_{ji} \right\} \leq \eta_{ji}, \quad \forall j, i, \quad (11c)$$

where,  $P_{si}$  is the allocated transmission power for SU  $s$  on subchannel  $i$ ,  $\mathbf{P}$  is a  $S \times N$  matrix,  $\mathbf{P} = [\mathbf{P}_1 | \dots | \mathbf{P}_S]$ , and  $\mathbf{P}_s = [P_{s1}, \dots, P_{sN}]^T$ . Constraint in (11b) ensures that the total transmit power in the SBS is always smaller than its maximum transmit power,  $P_T$ . Furthermore, (11c) keeps the collision probability for the PUs below  $\eta_{ji}$ . Hereafter, for brevity we assume the same QoS requirements for all users and over all subchannels, thus  $\beta_{ji} = \bar{\beta}$ , and  $\eta_{ji} = \bar{\eta}$ .

Obtaining the solutions of  $\mathcal{A}_1$  is challenged by the probabilistic constraint in (11c). Instead, similar to [19], we transform it to a convex approximation, assuming that the channel distribution information (CDI) of the interference channel,  $h_{ji}$ , is estimated at the SBS. Since there is often no direct signaling between the primary and secondary systems, estimating  $h_{ji}$ 's CDI based on the feedback from the PUs might not be an option. Therefore, other techniques such as the one in [19] might be adopted to estimate  $h_{ji}$  based on e.g., the level of interference signal. The constraint in (11c) is then

reduced to

$$\begin{aligned} \Pr \left\{ h_{ji} > \frac{\bar{\beta}}{\sum_{s=1}^S P_{si}} \right\} &= 1 - \Pr \left\{ h_{ji} \leq \frac{\bar{\beta}}{\sum_{s=1}^S P_{si}} \right\}, \\ &= 1 - F_{h_{ji}} \left[ \frac{\bar{\beta}}{\sum_{s=1}^S P_{si}} \right], \\ &\leq \bar{\eta}, \quad \forall j, i, \end{aligned} \quad (12)$$

where,  $F_X(x)$  is the cumulative distribution function (CDF) of random variable  $X$ .

### 1) RAYLEIGH DISTRIBUTED INTERFERENCE LINK

If  $h_{ji}$  follows a Rayleigh distribution with parameter  $r$ , then (12) is further reduced to

$$\exp \left( \frac{-\bar{\beta}}{2r^2 \sum_{s=1}^S P_{si}} \right) \leq \bar{\eta}, \quad \forall i. \quad (13)$$

For Rayleigh distributed  $h_{ji}$ , using (13), (11c) is then reduced to

$$\sum_{s=1}^S P_{si} \leq \frac{\bar{\beta}}{2r^2 \left( \ln \frac{1}{\bar{\eta}} \right)}, \quad \forall i. \quad (14)$$

Therefore,  $\mathcal{A}_1$  is converted to the following optimization problem:

$$\mathcal{A}_2 : \max_{\mathbf{P}} \sum_{s=1}^S \sum_{i=1}^N \frac{r_{si}}{\hat{\delta}_i} \alpha_{si}, \quad (15a)$$

$$\text{s.t.} \sum_{s=1}^S \sum_{i=1}^N P_{si} \leq P_T, \quad (15b)$$

$$\sum_{s=1}^S P_{si} \leq \frac{\bar{\beta}}{2r^2 \left( \ln \frac{1}{\bar{\eta}} \right)}, \quad \forall i. \quad (15c)$$

Hereafter, for brevity, we assume  $\alpha_{si} = 1 \forall i, s$ .

### 2) SUBOPTIMAL POWER ALLOCATION IN SBS

We note that  $\mathbf{P} \in \mathcal{P}$  is the feasible power allocation set in  $\mathcal{A}_2$  which is defined as  $\mathbf{P} = \mathcal{P}_1 \times \mathcal{P}_2 \times \dots \times \mathcal{P}_N$ , where  $\times$  is the Cartesian product. Since we have considered a multicell and multicarrier network, resource allocation jointly depends on PU's activity profile in neighbor base stations, and the QoS requirements of the SUs. Therefore,  $\mathbf{P}$  is directly dependent on the  $\delta_i$  from its neighbor base station, where  $\delta_i \in \{0, 1\}$ . Consequently  $\mathbf{P}$  is a non-convex solution set, therefore  $\mathcal{A}_2$  is a non-convex optimization problem.

Here, we adopt the dual decomposition approach [23], to obtain a suboptimal solution in optimization problem  $\mathcal{A}_2$ . There is a duality gap between the obtained solutions using dual decomposition method, and the actual optimal solutions. However, when the number of subchannels is sufficiently large, the duality gap becomes very small. Note that the obtained  $U_a$  using dual decomposition is in fact a lower bound on the maximum achieved total secondary system utility.

Lagrange function,  $\mathcal{L}$ , corresponding to  $\mathcal{A}_2$  is:

$$\begin{aligned} \mathcal{L}(\mathbf{P}, \lambda, \boldsymbol{\mu}) = & \sum_{i=1}^N \frac{1}{\hat{\delta}_i} \sum_{s \in \mathcal{S}} \log_2 \left( 1 + \frac{g_{si} P_{si}}{I_{pi} + N_0} \right) \\ & + \lambda \left( \sum_{s=1}^S \sum_{i=1}^N P_{si} \leq P_T \right) + \sum_{i=1}^N \mu_i \left( \sum_{s=1}^S P_{si} \leq \frac{\bar{\beta}}{2r^2 \left( \ln \frac{1}{\bar{\eta}} \right)} \right), \end{aligned} \quad (16)$$

where,  $\lambda \geq 0$  is the Lagrangian multiplier associated with the constraint (15b), and  $\boldsymbol{\mu} \geq 0$  is the Lagrangian vector associated with the constraints in (15c). The dual function is accordingly defined as:

$$\mathcal{D}(\lambda, \boldsymbol{\mu}) = \max_{\mathbf{P}} \mathcal{L}_a(P, \lambda, \boldsymbol{\mu}). \quad (17)$$

Therefore,

$$\begin{aligned} \mathcal{D}(\lambda, \boldsymbol{\mu}) = & \max_{\mathbf{P}} \sum_{i=1}^N \frac{1}{\hat{\delta}_i} \sum_{s \in \mathcal{S}} \log_2 \left( 1 + \frac{g_{si} P_{si}}{I_{pi} + N_0} \right) \\ & - \lambda \sum_{i=1}^N \sum_{s=1}^S P_{si} - \sum_{i=1}^N \mu_i \sum_{s=1}^S P_{si}, \end{aligned} \quad (18)$$

and thus the corresponding dual optimization problem is

$$\begin{aligned} & \min \mathcal{D}(\lambda, \boldsymbol{\mu}), \\ & \text{s.t. } \lambda \geq 0, \quad \boldsymbol{\mu} \geq 0. \end{aligned} \quad (19)$$

The optimal transmission power obtained from (19) maximizes the total system utility, however it needs to adjust  $\lambda$ ,  $\boldsymbol{\mu}$ , which are in fact the prices associated with the violation of constraints in  $\mathcal{A}_2$ .

Here, Lagrangian multipliers ( $\lambda$ ,  $\boldsymbol{\mu}$ ) are iteratively estimated using the sub-gradient method [24], where the suitable direction of ( $\lambda$ ,  $\boldsymbol{\mu}$ ) is obtained. This reduces the computational complexity of finding the solution of the optimization problem. The value of  $\lambda$  and  $\boldsymbol{\mu}$  are calculated through the following iterations:

$$\begin{aligned} \lambda(n+1) &= \left( \lambda_i(n) + \Delta_s(n) \left( P_T - \sum_{s=1}^S \sum_{i=1}^N P_{si} \right) \right)^+, \quad (20) \\ \mu_i(n+1) &= \left( \mu_i(n) + \Delta_s(n) \left( \frac{\bar{\beta}}{2r^2 \left( \ln \frac{1}{\bar{\eta}} \right)} - \sum_{s=1}^S P_{si} \right) \right)^+, \end{aligned} \quad (21)$$

where,  $(a)^+ = \max\{0, a\}$  and  $\Delta_s(n)$  is the step size at the  $n^{\text{th}}$  iteration. The step size is initialized as  $\Delta_s(n) \geq 0$ , where  $\sum_{n=1}^{\infty} \Delta_s^2(n) < \infty$ , and  $\sum_{n=1}^{\infty} \Delta_s(n) \rightarrow \infty$ . Here, we dynamically update the step size,  $\Delta_s(n)$ , towards the convergence. This will reduce the number of iterations to find the optimal solution.

The optimal power allocation for each subchannel which maximizes the total utility in the SBS is a classic water-filling

problem, see [23], thus,

$$P_{si}^* = \left( \frac{1/\ln(2)}{\hat{\delta}_i(\lambda + \sum_i \mu_i)} - \frac{I_{pi} + N_0}{g_{si}} \right)^+. \quad (22)$$

As it is seen, (22) returns  $P_{si}^* = 0$  for subchannel  $i$  if  $\frac{I_{pi} + N_0}{g_{si}} > \frac{1/\ln(2)}{\hat{\delta}_i(\lambda + \sum_i \mu_i)}$ ,  $\forall s$ . Note that  $P_{si}^*$  is independent from  $\bar{\eta}$  and  $\bar{\beta}$ . Therefore, the constraint in (15c) needs to be re-evaluated as a further requirement of suboptimal transmit power.

In OFDMA based cognitive radio systems only one SU,  $s^*$ , accesses subchannel  $i$ , therefore the maximum transmission power for the case where there is a free subchannel is calculated as the maximum value of the constraint in (15c):

$$P_{s^*i}^* = \frac{\bar{\beta}}{2r^2 \left( \ln \frac{1}{\bar{\eta}} \right)}. \quad (23)$$

Therefore, the optimum transmission power is

$$P_{si}^{opt} = \min \{ \max(0, P_{si}^*), \max(P_{s^*i}^*, 0) \}, \quad \forall s, i, \quad (24)$$

which maintains the collision probability requirement for all the PUs as well as the transmission power constraint for the SBSs. Eq. (24) is in fact the minimum value of (22) and (23), which is considered as the optimal transmission power because this does not violate other constraints and also fulfills the QoS requirements of the primary system. To speed up the convergence rate and reduce the computational complexity, one may consider  $\varepsilon$ -suboptimality, where the level of computational complexity is inversely related to  $\varepsilon^2$ .

#### IV. ENERGY EFFICIENT POWER ALLOCATION

In this section, the efficient transmission power allocation method is investigated from the energy efficiency perspective. As mentioned in the previous section, the ASAI provides an extra degree of freedom in system design to achieve the optimal spectral efficiency. Here, we study the implication of  $\hat{\delta}_i$  on the EE of the CRN as a new design criteria. We extend the objective function and accordingly define it as the achievable utility per unit power. Similar to the case of spectral efficiency, we consider the total interference constraints to guarantee the minimum QoS to the PUs. Therefore, we define a utility function  $U_b$  to characterize the energy efficiency of the system:

$$U_b = \frac{\sum_{i=1}^N \frac{1}{\hat{\delta}_i} \sum_{s \in \mathcal{S}} \log_2 \left( 1 + \frac{g_{si} P_{si}}{I_{pi} + N_0} \right)}{k_1 + k_2 \sum_{i=1}^N \sum_{s=1}^S P_{si}} \alpha_{si}, \quad (25)$$

where,  $k_1$  and  $k_2$  are the circuit operation power and power amplifier consumptions, respectively. For brevity hereafter we assume  $\alpha_{si} = 1$ ,  $\forall i, s$ .



The maximum achievable EE is then obtained through the following optimization problem.

$$\mathcal{A}_3 : \xi^* = \max_{\mathbf{P}} \frac{\sum_{i=1}^N \frac{1}{\hat{\delta}_i} \sum_{s \in S} \log_2 \left( 1 + \frac{g_{si} P_{si}}{I_{pi} + N_0} \right)}{k_1 + k_2 \sum_{i=1}^N \sum_{s=1}^S P_{si}}, \quad (26a)$$

$$\text{s.t. } \sum_{s=1}^S P_{si} h_{ji} < \beta_{ji}, \quad (26b)$$

$$P_{si} \geq 0 \quad \forall s, i, \quad (26c)$$

$$P_{si} \leq P_{max} \quad \forall s, i. \quad (26d)$$

The optimization problem in  $\mathcal{A}_3$  needs to be approximated to be transformed into a convex optimization problem. We show that the fractional function in (26a) requires further analysis to show that it is quasi-concave. Subject to the KKT conditions, we then conclude that  $P_{s,i}^*$  is an optimal solution, see [11] and references therein.

We use the results in [25] in which it is shown that utilizing Charnes-Cooper Transformation (CCT), a quasi-concave fractional optimization problem can be further reduced to a concave optimization problem. To further simplify  $\mathcal{A}_3$ , here we define auxiliary variables,  $y$ , and  $t$ , where  $y = tP$ , i.e.,  $P = \frac{y}{t}$ , and  $t = \frac{1}{k_1 + k_2 \sum_{i=1}^N \sum_{s=1}^S P_{si}}$ , and  $y \triangleq \{y_{si}\}_{s=1 \dots S, i=1 \dots N}$ .

As it is seen,  $y_{si}$  is proportional to the allocated power to SU,  $s$  on subchannel  $i$ . Further analytical manipulation,  $\mathcal{A}_3$  is then reduced as follows.

$$\mathcal{A}_4 : \max_{y, t > 0} t \sum_{i=1}^N \frac{1}{\hat{\delta}_i} \sum_{s \in S} \log_2 \left( 1 + \frac{y}{t} \frac{g_{si}}{I_{pi} + N_0} \right), \quad (27a)$$

$$\text{s.t. } \sum_{s=1}^S y_{si} g_j - \bar{\beta} t \leq 0, \quad (27b)$$

$$t \left( k_1 + k_2 \sum_{i=1}^N \sum_{s=1}^S y_{si} \right) = 1, \quad (27c)$$

$$y_{si} \geq 0 \quad \forall s, i. \quad (27d)$$

Here, we note that  $t$  appears in numerator of the objective function as well as in the denominator of the second term of the objective function. Therefore,  $\mathcal{A}_4$  can be further reduced as follows.

$$\mathcal{A}_5 : \max_{y, t > 0} \sum_{i=1}^N t \frac{1}{\hat{\delta}_i} \sum_{s \in S} \log_2 \left( t + y \frac{g_{si}}{I_{pi} + N_0} \right) - \sum_{s=1}^S \frac{1}{\hat{\delta}_i} t \log_2(t), \quad (28a)$$

$$\text{s.t. } (27b), (27c), (27d). \quad (28b)$$

The Lagrangian function corresponding to  $\mathcal{A}_5$  is

$$\begin{aligned} \mathcal{L}(\mathbf{y}, t, \lambda, \mu, \phi, \nu) &= \sum_{i=1}^N t \frac{1}{\hat{\delta}_i} \sum_{s \in S} \log_2 \left( t + y \frac{g_{si}}{I_{pi} + N_0} \right) \end{aligned}$$

**Algorithm 2** Iterative Power Allocation Algorithm and EE Optimization

**Input:** error tolerance:  $\varepsilon > 0$ , maximum iterations:  $I_{max}$ , iteration index:  $n$ ,  $\lambda^{(0)} = \lambda_{(0)}$ ,  $\mu^{(0)} = \mu_{(0)}$ , initial EE:  $\xi^{(0)} = \xi_{(0)}$

**Output:**  $\varepsilon$ -optimal power profile:  $\mathbf{P}^*$ , optimal EE:  $\xi^*$

- 1: **while** ( $n \leq I_{max}$  AND  $X_{\mathcal{N}}(\mathbf{P}^*, \hat{\delta}_i) - \xi^* X_{\mathcal{D}}(\mathbf{P}^*, \hat{\delta}_i) \geq 0$ ) **do**
- 2:     obtain  $\mathbf{P}^{(n)}$  from (30) for a given (or obtained)  $\xi^{(n)}$
- 3:     obtain  $\lambda^{(n)}$ , and  $\mu^{(n)}$  using subgradient method
- 4:     set  $n = n + 1$ , and  $\xi^{(n)} = \frac{X_{\mathcal{N}}(\mathbf{P}^*, \hat{\delta}_i)}{X_{\mathcal{D}}(\mathbf{P}^*, \hat{\delta}_i)}$
- 5: **end while**
- 6: **return** the  $\varepsilon$ -optimal power allocation profile  $\mathbf{P}^* = \mathbf{P}^{(n)}$ , and  $\xi^* = \xi^{(n)}$ .

$$\begin{aligned} & - \sum_{s=1}^S \frac{1}{\hat{\delta}_i} t \cdot \log_2(t) - \sum_{i=1}^N \lambda_i \left( \sum_{s=1}^S y_{si} g_j - \bar{\beta} t \right) \\ & - \mu \left( t \cdot k_1 + k_2 \sum_{i=1}^N \sum_{s=1}^S y_{si} - 1 \right) + \sum_{s=1}^S \phi_s y_s + \nu \cdot t, \end{aligned} \quad (29)$$

where,  $\lambda$ ,  $\mu$ ,  $\phi$  and  $\nu$  are Lagrangian coefficients associated with the corresponding constraints in  $\mathcal{A}_5$ . In addition,  $\xi$  can also be defined as EE and we find optimal transmission power profile which maximizes  $\xi$ . Following the same line of arguments as in the Section III, by taking the complimentary slackness of KKT condition and noting that  $0 \leq \mathbf{P} \leq P_{max}$ , where  $P_{max}$  is the maximum limit of transmit power, we then find the optimal transmission power,  $P^* = \frac{y^*}{t^*}$  as:

$$P_{si}^* = \min \left\{ \left[ \frac{\frac{1}{\ln(2)}}{\hat{\delta}_i (\sum_i \lambda_i g_j + \mu)} - \frac{I_{pi} + N_0}{g_{si}} \right]^+, P_{max} \right\}. \quad (30)$$

A new optimization problem can also be obtained by adding a new constraint to the total transmission power in  $\mathcal{A}_5$ . The closed form solution of the optimal transmission power can be obtained similar to (30). Therefore,  $P_{max}$  has been considered as the maximum of  $P_{si}^*$ . For detail analysis of such scenario, refer to, e.g., [26] and references therein.

For further observation, we write the fractional utility function,  $U_b$ , in (25) as  $\xi = \frac{X_{\mathcal{N}}(\mathbf{P}, \hat{\delta}_i)}{X_{\mathcal{D}}(\mathbf{P}, \hat{\delta}_i)}$ . Optimal value of  $\xi$  and transmit power are then obtained by utilizing the *Dinkelbach's Theorem* [27] as follows.

*Theorem 2: The optimal EE,  $\xi^*$ , is achieved if*

$$\begin{aligned} \max_{\mathbf{P}} \{X_{\mathcal{N}}(\mathbf{P}, \hat{\delta}_i) - \xi^* X_{\mathcal{D}}(\mathbf{P}, \hat{\delta}_i)\} \\ = X_{\mathcal{N}}(\mathbf{P}^*, \hat{\delta}_i) - \xi^* X_{\mathcal{D}}(\mathbf{P}^*, \hat{\delta}_i) = 0 \end{aligned}$$

*is satisfied for  $X_{\mathcal{N}}(\mathbf{P}, \hat{\delta}_i) \geq 0$ , and  $X_{\mathcal{D}}(\mathbf{P}, \hat{\delta}_i) > 0$ .*

Based on Theorem 2, we then develop an iterative algorithm to obtain the optimal power allocation for each subchannel,  $\mathbf{P}^*$ , based on (30) which is also EE optimal.

TABLE 1. Simulation parameters.

Number of subchannels ( $N$ )	32
subchannel Bandwidth ( $B_i$ )	125 KHz
Channel Model	Rayleigh with $r = 1$
Number of The Secondary Users ( $S$ )	6
Interference Threshold ( $\beta$ )	0.15
Collision Probability Threshold ( $\bar{\eta}$ )	0.1 – 0.6
Maximum SBS Transmit Power ( $P_T$ )	10-30 dBm
Probability of Idle subchannel ( $P_{H0}$ )	0.5
Thermal Noise Density	-174 dBm/Hz

According to Theorem 2, the transmit power is optimal if in Algorithm 2,  $X_{\mathcal{N}}(\mathbf{P}^*, \hat{\delta}_i) - \xi^* X_{\mathcal{D}}(\mathbf{P}^*, \hat{\delta}_i)$  is equal to zero after  $n$  iterations. To reduce the number of iterations, we consider  $\varepsilon$ -optimal power allocation, therefore,  $X_{\mathcal{N}}(\mathbf{P}^*, \hat{\delta}_i) - \xi^* X_{\mathcal{D}}(\mathbf{P}^*, \hat{\delta}_i) < \varepsilon$ , where  $\varepsilon > 0$  is the error tolerance. The convergence of Algorithm 2 depends on the associated constraints, channel state information, and error tolerance in the secondary system.

V. SIMULATION RESULTS

A. SIMULATION SETTINGS

In this section, we perform the simulation on an OFDMA based cellular CRN as shown in Fig. 1. First, we consider one base station, e.g., SBS0, which implements the proposed Algorithm 1 presented in Section III. Both primary and secondary users are randomly dispersed within the transmission range of SBS0. In each time frame, ASAI, i.e.,  $0 < \hat{\delta}_i \leq 1$ , where  $i \in \{1, \dots, N\}$ , is estimated. As mentioned in the previous sections, ASAI in all subchannels are independently estimated through the collaborative energy detection method. The path-loss exponent is assumed to be 2.7 and shadowing follows log-normal distribution, normalized to have mean one and standard deviation of 7.5 dB. The simulation parameters are shown in Table 1, unless otherwise stated. Note that, the decision variable which is the received SNR for spectrum sensor as shown in (6) has been obtained under equiprobable hypothesis channel for mathematical tractability, see Appendix A and [28]. It is therefore assumed that the subchannels are equiprobable and  $P_{H0} = 0.5$ .

We investigate the impact of system parameters on the performance of the proposed method. We then compare the system performance of the proposed method with two benchmark systems. Various schemes have been proposed in literature to measure the performance of channel and power allocation technique, e.g., [5], [29], [30]. To the best of our knowledge, there are however no directly related works in multicell cognitive environment in which the collaborative spectrum sensing results are utilized in decision making process for resource allocation. Based on the available literature, several benchmark models have been developed for comparison. The concepts of equal power allocation, perfect channel utilization, and bursty primary traffic are designed from the previous works for comparison purpose in this paper. They are considered to be upper and lower bounds for the

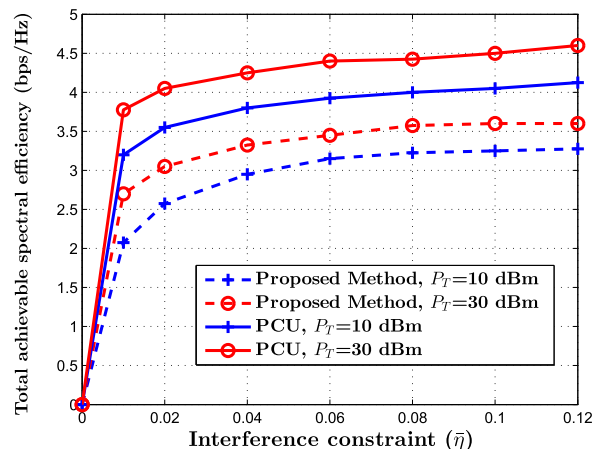


FIGURE 3. Total achievable spectral efficiency of the SBS vs. collision probability threshold, for  $P_T = 10, 30$  dBm for the proposed method and the PCU for  $\hat{\delta} = 0.6$ .

performance measurement. The primary purpose of the proposed performance comparison is to measure how close it is with the upper-bound result and the performance gain compared to the lower-bound. In cases where the performance of the proposed method is closer to that of the ideal scenario, the more efficient will be the radio resource allocation technique.

The first one is referred to as *Equal Power Allocation* (EPA). Here, EPA is the scenario under which stand-alone SBS0 with no signaling among the adjacent SBSs is considered. As a result, base station does not have any knowledge of ASAI which ultimately forces to allocate equal power in all the subchannels. Moreover, *Perfect Channel Utilization* (PCU) is considered as a second reference model for comparison. This ideal scenario is the upper-bound benchmark, which is generally not available in practice. Here, PCU is a scenario in which an ideal spectrum sharing system is considered, where both accurate spectrum sensing information and perfect interference channel state are available on the secondary system. PCU utilizes overlay spectrum sharing for idle subchannels, and underlay spectrum sharing method for underutilized subchannels.

For underlay method, the secondary system SE is maximized for a proposed power allocation method subject to aggregated interference constraint and maximum SBS transmit power. Moreover, EPA can be considered as a worst case scenario due to the lack of knowledge about primary user activity and interference channel status, whereas PCU is considered as the best case scenario due to the availability of interference channel and user activity information. The investigated performance metric is the total achievable spectral efficiency defined as  $\sum_{s=1}^S \sum_{i=1}^N r_{si}$  which is the sum-rate normalized over the system bandwidth.

B. IMPACT OF COLLISION PROBABILITY CONSTRAINT

The achievable SE at the SBS versus  $\bar{\eta}$  is plotted in Fig. 3 for the proposed power allocation scheme as well as the system settings for PCU. As expected, allocating a higher

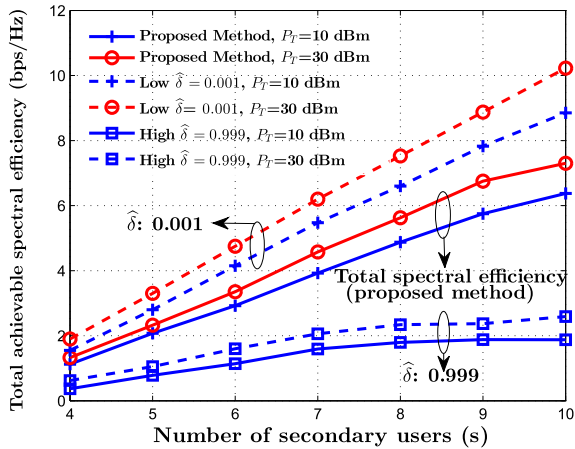


FIGURE 4. Total achievable spectral efficiency of the SBS vs. the number of SUs,  $S$ , for  $P_T = 10, 30$  dBm,  $\hat{\delta} = 0.001, 0.6$ , and  $\bar{\eta} = 0.05$ .

maximum transmission power results in a higher SE. We further observe that increasing  $P_T$  from 10 to 30 dBm results in an improvement of 0.5 bps/Hz on SE mostly in all considered interference constraint from 0.01 to 0.12. Corresponding to a larger  $P_T$ , a relatively greater throughput improvement is observed for larger values of  $\bar{\eta}$ . Since a primary system with a larger  $\bar{\eta}$  demonstrates a higher tolerance against the secondary interference, the SBS is able to allocate a higher transmission power and achieves a higher SE.

Fig. 3 further indicates that the SE performance of the proposed method closely follows the scenario of PCU. Note that comparing to PCU, the proposed method requires a significantly lower signaling overhead. In other words, the lower level of required signaling in the proposed method is associated with a reasonable cost on throughput.

Here, the achievable spectral efficiency of the proposed method for two distinct primary network load conditions are compared. The first scenario is the case in which the primary service transmitter has very limited amount of data to transmit. This situation is modeled by setting very low duty cycle which apparently simulates the low traffic intensity at primary transmitter. This will result a very low ASAI which is obtained, in average, at  $\hat{\delta} = 0.001$ . The next is a case where moderately loaded primary service is considered, where subchannel activity index is approximately achieved to be  $\hat{\delta} = 0.6$ . The case when  $\hat{\delta} = 0.001$  is obtained, the power allocation in Section III acts similar to an overlay method of spectrum access. Therefore, the comparison presented here indicates how efficient is the proposed power allocation scheme in exploiting the load variations in the primary network.

The total achievable spectral efficiency in the secondary system is plotted in Fig. 4 when the number of SUs ( $S$ ) varies in the range of 4 to 10, and total transmit power ( $P_T$ ) varies from 10 to 30 dBm. Also the network scenario is maintained such that ASAI is approximately estimated to be  $\hat{\delta} = 0.001, 0.6, 0.999$ , and  $\bar{\eta} = 0.05$ . As it is observed

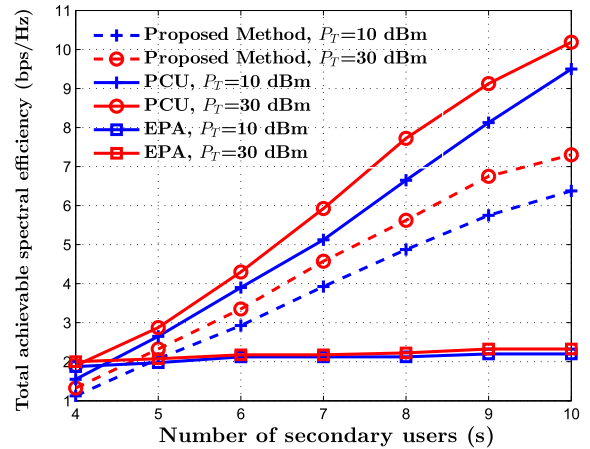


FIGURE 5. Total achievable spectral efficiency of the secondary system vs. the total number of the secondary users, for different scenarios and  $P_T$  values.

in Fig. 4, by increasing ASAI ( $\hat{\delta}_i$ ) in the primary network, the achievable SE at the secondary system is decreased. Surprisingly however, the achievable SE of the proposed method is very close to that of the overlay access for a low to moderate secondary network load. It is also observed in Fig. 4 that for  $P_T = 10, 30$  dBm, the spectral efficiency does not increase in the same rate. This is due to the imposed collision probability constraint in the optimization problem.

C. COMPARISON WITH EPA and PCU

The SE of the proposed system along with its comparison against two benchmark power allocation settings, i.e., EPA and PCU, are presented in Fig. 5. The variations in traffic demand in the secondary system represented by the number of SUs,  $S$ . As expected, PCU achieves the highest system utility, whereas EPA has the lowest. The proposed resource allocation scheme however achieves a significantly higher SE than that of the EPA. This is due to the fact that the primary system activity provided by incorporating ASAI is exploited in the subchannel power allocation. It is further observed that the proposed method closely follows the ideal subchannel access, i.e., PCA with a slightly lower SE but significantly lower signaling overhead among the SBSs.

D. IMPACT OF PRIMARY NETWORK TRAFFIC ON ENERGY EFFICIENCY

We now compare the performance of the proposed method in terms of EE against the case when the ASAI is not estimated. In cases where the impact of interference from primary system increases, the achievable energy efficiency deteriorates due to the higher transmit power requirement at the secondary system to suppress the interference. The lowest EE is achieved when the primary network traffic is of bursty nature in which the variation of  $\hat{\delta}$  becomes high. Therefore, even in the lower interference regime, the EE is not significantly higher. For instance, EE is achieved to be four times higher ( $\approx 20$  b/Hz/Joule) when  $\hat{\delta} = 0.7$  than the case of

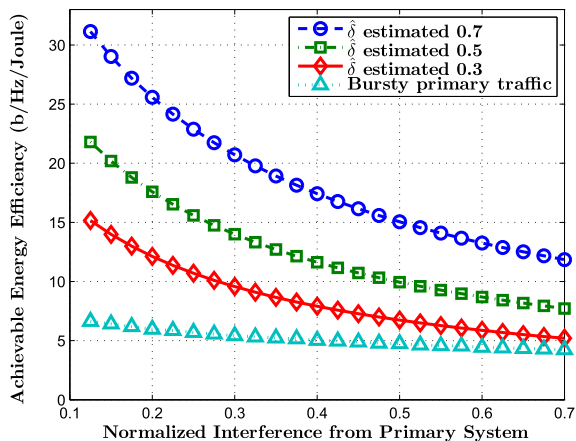


FIGURE 6. Energy efficiency vs. normalized interference from primary system for various primary network traffic.

bursty primary network traffic ( $\approx 5$  b/Hz/Joule). Therefore, it can be concluded that the  $\hat{\delta}$  estimation enables the improved resource allocation to achieve higher EE as shown in Fig. 6.

Moreover, in cases with perfect primary user activity estimation, by increasing the primary users activity there are more opportunities available to access the subchannels such that the system energy is significantly utilized for data transmission to achieve improved EE. In cases where the interference from the primary system is higher, energy efficiency cannot be significantly improved. For instance at the normalized interference of 0.6, the EE is improved from 4 to 6 b/Hz/Joule, for cases of bursty primary traffic, and  $\hat{\delta}_i = 0.3$ , respectively.

**E. ENERGY EFFICIENCY AND TOTAL SPECTRAL EFFICIENCY**

When the PUs are highly active by accessing the subchannels more frequently, i.e., higher  $\hat{\delta}_i$ , the achievable rate at SBS is decreased as shown in Fig. 7. Interestingly, however, it is observed that when smaller number of the PUs accessing their subchannel is reduced, e.g.,  $\hat{\delta}_i < 0.5$ , increasing  $P_T$  does not significantly improve better system throughput. As it is seen, the increase in  $P_T$  from 10 dBm to 30 dBm, the maximum SE achievement is below 1 bps/Hz. This is due to the fact that, for lower  $\hat{\delta}$ , where a large number of subchannels are available for secondary system, per subchannel transmit power at SBS remains almost constant even where higher  $P_T$  is allocated due to the imposed interference constraint.

Here, we further analyze the optimal EE and SE as a unified model for the real-time measurement of the subchannel activity index,  $\hat{\delta}$ , since both EE and SE depend on optimal transmit power and QoS requirements imposed by the primary system. In addition, the ASAI is used in the proposed analytical models to design the optimal transmit power allocation.

The optimal SE and EE as a function of  $\hat{\delta}_i$  for the proposed method, for a range of total transmit power, is shown in Fig. 7. The proposed methods improve the performance in various range of ASAI, i.e.,  $\hat{\delta}_i$ . It is shown in Fig. 7, for instance, that

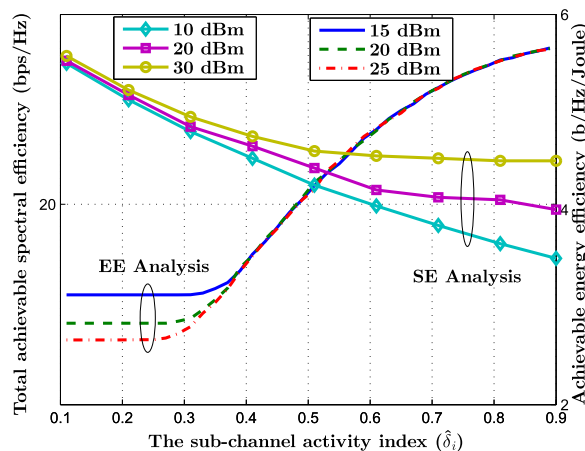


FIGURE 7. Achievable spectral and energy efficiency vs. primary user activity index for various total power constraints.

when subchannels are busy, as indicated by  $\hat{\delta}_i$  in the range of [0.65, 0.9], the transmission power is controlled in such a way that the EE is improved whereas the SE does not degrade significantly when maximum  $P_T$  is 30 dBm. Also in the lower ASAI, as indicated by  $\hat{\delta}_i$  in the range of [0.1, 0.3], EE remains in the same level of around 15 b/Hz/Joule without significant decrease in SE. Moreover, when the primary channels are moderately occupied, i.e.,  $\hat{\delta}_i$  in the range of [0.4, 0.6], the secondary system can achieve an acceptable levels of both EE and SE simultaneously. As it is seen, in this case, the maximum  $P_T$  does not play a vital role on the system performance.

In a conventional EE and SE optimization, the improvement in EE as well as SE is obtained either by considering a linear combination of EE and SE objectives [31], or defining an objective function based on the transmit power as discussed in [13]. In such cases, when the transmit power is increased, improved SE is obtained with the sacrifice on the EE and vice-versa. The major concern in such models of CRN design is that there is a limited range of transmit power for SUs due to the interference constraints imposed by primary system. For instance, the higher the transmit power, larger will be the interference to the primary system which puts the transmit power restrictions on the secondary transmitters. In our proposed model however, relaxing (or tightening) the constraint in (6) by fine-tuning radio sensing parameters, larger (or smaller) number of subchannels are available for SUs such that  $\hat{\delta}_i$  slightly adjusts to the higher (or lower) range. Therefore, depending on the requirements, i.e., either better EE or better SE is anticipated, the mobile network operators can optimize the system parameters to achieve the optimized EE or SE, as shown in Fig. 7, without compromising the QoS on primary system.

Therefore, the proposed method provides an entirely new perspective on cognitive communication and network design, where the operating point in terms of ASAI, as shown in x-axis in the Fig. 7, can be dynamically obtained by adjusting

the spectrum sensing related parameters, e.g., sensing duration, sensing threshold, and detection probability threshold.

**F. APPLICATION FRAMEWORK**

The cyber-physical system (CPS) connects our physical world to the information world by integrating the technologies like IoT, M2M, cellular network, fog computing etc. to our daily life. The proposed method of radio resource allocation, nevertheless, has applications within the CPS framework, for instance, manufacturing, e-health, military systems, traffic control, physical security and many more. For such applications, we need significantly larger number of real-time sensing data which are processed to efficiently interact with the real-world problems. On the other hand, the devices must be highly energy efficient to operate for longer duration without changing the battery sources. The distributed sensing and resource allocation techniques proposed in this paper aims to significantly contribute to enable such CPS technologies by providing a degree of freedom to control EE and SE through spectrum sensing parameters.

**VI. CONCLUSION AND FUTURE WORK**

In this paper, we proposed and characterized SAI to incorporate the communication activity associated with the PUs in efficient resource allocation. We then proposed a simple yet efficient collaborative spectrum monitoring scheme with very low signaling overhead to evaluate the activities level of users in the subchannels, i.e., ASAI, as an indicator of network wide activities level of PUs on the subchannels. We then obtained the efficient power allocation profile at the SBS with the objective of maximizing total SBS utility, defined based on ASAI. We also investigated the impact of ASAI into the EE by defining the utility function and obtained the efficient transmit power profile. A practically viable design between SE and EE was successfully achieved considering the primary communication activity on the allocated subchannels. Simulation results confirmed that the proposed scheme exploited the variations in the primary system communication activity to improve the secondary system achievable rate. We also investigated the impact of ASAI into the EE and concluded that the proposed method is a better design approach to obtain the optimal EE and SE concurrently by adjusting the spectrum sensing parameters. As a future work, we investigate the impact of proposed radio resource allocation in machine type communication (MTC) network and compare its performance against recent technologies, e.g., *LoRa*, *SigFox* and *Narrowband-IoT* standard.

**APPENDIX A  
PROOF OF THEOREM 1**

*Proof:* Based on the spectrum sensing result, the subchannel is estimated to be busy if the following condition is satisfied.

$$\frac{(1 - \mathcal{P}_{fa,i})\Pr(H_0) + \mathcal{P}_{md,i}\Pr(H_1)}{(1 - \mathcal{P}_{md,i})\Pr(H_1) + \mathcal{P}_{fa,i}\Pr(H_1)} < 1. \tag{31}$$

The false alarm probability is bounded by its maximum threshold at  $\bar{\mathcal{P}}_{fa,i}$  which is a system defined parameter, for instance IEEE WRAN 802.22 [21], where  $\bar{\mathcal{P}}_{fa,i} \leq 10\%$ . Therefore,

$$\frac{(1 - \bar{\mathcal{P}}_{fa,i})\Pr(H_0) + Q\left(\left(\frac{\varepsilon_i}{\sigma_w^2} - \gamma_i - 1\right)\sqrt{\frac{T_{if0}}{2\gamma_i + 1}}\right)\Pr(H_1)}{(1 - Q\left(\left(\frac{\varepsilon_i}{\sigma_w^2} - \gamma_i - 1\right)\sqrt{\frac{T_{if0}}{2\gamma_i + 1}}\right))\Pr(H_1) + \bar{\mathcal{P}}_{fa,i}\Pr(H_1)} < 1. \tag{32}$$

Here, we assume equiprobable hypothesis over subchannels as in [28] for mathematical tractability in which the probability of a subchannel being idle is equal to that of being busy. However, the result is equally valid for all other scenarios with slide modification on the result. The condition to avoid the subchannel due to its unavailability is then obtained as

$$\frac{(1 - \bar{\mathcal{P}}_{fa,i}) + Q\left(\left(\frac{\varepsilon_i}{\sigma_w^2} - \gamma_i - 1\right)\sqrt{\frac{T_{if0}}{2\gamma_i + 1}}\right)}{(1 - Q\left(\left(\frac{\varepsilon_i}{\sigma_w^2} - \gamma_i - 1\right)\sqrt{\frac{T_{if0}}{2\gamma_i + 1}}\right)) + \bar{\mathcal{P}}_{fa,i}} < 1, \tag{33}$$

this can be reduced to

$$1 - \bar{\mathcal{P}}_{fa,i} - Q\left(\left(\frac{\varepsilon_i}{\sigma_w^2} - \gamma_i - 1\right)\sqrt{\frac{T_{if0}}{2\gamma_i + 1}}\right) < 1. \tag{34}$$

Straightforward mathematical manipulations results in

$$\frac{Q^{-1}(1 - \bar{\mathcal{P}}_{fa,i})}{\sqrt{T_{if0}}} > \left(\frac{\varepsilon_i}{\sigma_w^2} - 1\right) \frac{1}{\sqrt{2\gamma_i + 1}} - \frac{\gamma_i}{\sqrt{2\gamma_i + 1}}, \quad \forall i. \tag{35}$$

Setting  $\Theta_{1i} = \frac{\varepsilon_i}{\sigma_w^2} - 1$ ,  $\Theta_{2i} = \frac{Q^{-1}(1 - \bar{\mathcal{P}}_{fa,i})}{\sqrt{T_{if0}}}$ , (35) is further reduced to

$$\gamma_i > \Theta_{1i} + \Theta_{2i}^2 \pm \Theta_{2i}\sqrt{\Theta_{2i}^2 + 2\Theta_{1i} + 1}, \quad \forall i. \tag{36}$$

Similarly, the subchannel is estimated to be busy where the following condition is satisfied:

$$\frac{(1 - \mathcal{P}_{fa,i})\Pr(H_0) + \mathcal{P}_{md,i}\Pr(H_1)}{(1 - \mathcal{P}_{md,i})\Pr(H_1) + \mathcal{P}_{fa,i}\Pr(H_1)} > 1. \tag{37}$$

Following the same lines of arguments as above, we then obtain spectrum sensing decision threshold as

$$\gamma_i < \Theta_{1i} + \Theta_{2i}^2 \pm \Theta_{2i}\sqrt{\Theta_{2i}^2 + 2\Theta_{1i} + 1}, \quad \forall i. \tag{38}$$

The detection criteria for spectrum availability is considered for the best possible SNR at the energy detector is

$$\gamma_i \geq \max\{\Theta_{1i} + \Theta_{2i}^2 \pm \Theta_{2i}\sqrt{\Theta_{2i}^2 + 2\Theta_{1i} + 1}\}, \quad \forall i, \tag{39}$$

which completes the proof. ■

## REFERENCES

- [1] I. Kakalou, K. E. Psannis, P. Krawiec, and R. Badae, "Cognitive radio network and network service chaining toward 5G: Challenges and requirements," *IEEE Commun. Mag.*, vol. 55, no. 11, pp. 145–151, Nov. 2017.
- [2] M. Khoshkholgh, K. Navaie, and H. Yanikomeroglu, "Achievable capacity in hybrid DS-CDMA/OFDM spectrum-sharing," *IEEE Trans. Mobile Comput.*, vol. 9, no. 6, pp. 765–777, Jun. 2010.
- [3] Deepak G. C. and K. Navaie, "A low-latency zone-based cooperative spectrum sensing," *IEEE Sensors J.*, vol. 16, no. 15, pp. 6028–6042, Aug. 2016.
- [4] P. Mach and Z. Bencvar, "Energy-aware dynamic selection of overlay and underlay spectrum sharing for cognitive small cells," *IEEE Trans. Veh. Technol.*, vol. 66, no. 5, pp. 4120–4132, May 2017.
- [5] G. Bansal, M. Hossain, V. Bhargava, and T. Le-Ngoc, "Subcarrier and power allocation for OFDMA-based cognitive radio systems with joint overlay and underlay spectrum access mechanism," *IEEE Trans. Veh. Technol.*, vol. 62, no. 3, pp. 1111–1122, Mar. 2013.
- [6] L. Liu, R. Zhang, and K.-C. Chua, "Achieving global optimality for weighted sum-rate maximization in the K-user gaussian interference channel with multiple antennas," *IEEE Trans. Wireless Commun.*, vol. 11, no. 5, pp. 1933–1945, May 2012.
- [7] J. Zou, H. Xiong, D. Wang, and C. W. Chen, "Optimal power allocation for hybrid overlay/underlay spectrum sharing in multiband cognitive radio networks," *IEEE Trans. Veh. Technol.*, vol. 62, no. 4, pp. 1827–1837, May 2013.
- [8] Deepak G. C., K. Navaie, and Q. Ni, "Inter-cell collaborative spectrum monitoring for cognitive cellular networks in fading environment," in *Proc. IEEE Int. Conf. Commun. (ICC)*, Jun. 2015, pp. 7498–7503.
- [9] J. Ouyang, M. Lin, Y. Zou, W.-P. Zhu, and D. Massicotte, "Secrecy energy efficiency maximization in cognitive radio networks," *IEEE Access*, vol. 5, pp. 2641–2650, Feb. 2017.
- [10] X. Hong, J. Wang, C.-X. Wang, and J. Shi, "Cognitive radio in 5G: A perspective on energy-spectral efficiency trade-off," *IEEE Commun. Mag.*, vol. 52, no. 7, pp. 46–53, Jul. 2014.
- [11] A. Alabbasi, Z. Rezki, and B. Shihada, "Energy efficient resource allocation for cognitive radios: A generalized sensing analysis," *IEEE Trans. Wireless Commun.*, vol. 14, no. 5, pp. 2455–2469, May 2015.
- [12] S. Wang, W. Shi, and C. Wang, "Energy-efficient resource management in OFDM-based cognitive radio networks under channel uncertainty," *IEEE Trans. Commun.*, vol. 63, no. 9, pp. 3092–3102, Sep. 2015.
- [13] W. Zhang, C. Wang, D. Chen, and H. Xiong, "Energy-spectral efficiency tradeoff in cognitive radio networks," *IEEE Trans. Veh. Technol.*, vol. 65, no. 4, pp. 2208–2218, Apr. 2015.
- [14] L. Wang, M. Sheng, Y. Zhang, X. Wang, and C. Xu, "Robust energy efficiency maximization in cognitive radio networks: The worst-case optimization approach," *IEEE Trans. Commun.*, vol. 63, no. 1, pp. 51–65, Jan. 2015.
- [15] F. Kelly, "Charging and rate control for elastic traffic," *Eur. Trans. Telecommun.*, vol. 8, no. 1, pp. 33–37, Jan./Feb. 1997.
- [16] M. Katoozian, K. Navaie, and H. Yanikomeroglu, "Utility-based adaptive radio resource allocation in OFDM wireless networks with traffic prioritization," *IEEE Trans. Wireless Commun.*, vol. 8, no. 1, pp. 66–71, Jan. 2009.
- [17] J. Kaleva, A. Tolli, and M. Juntti, "Weighted sum rate maximization for interfering broadcast channel via successive convex approximation," in *Proc. IEEE GLOBECOM*, Dec. 2012, pp. 3838–3843.
- [18] M. Soleimanpour-Moghadam and S. Talebi, "Jointly optimal rate control and total transmission power for cooperative cognitive radio system," *IET Commun.*, vol. 11, no. 11, pp. 1679–1688, 2017.
- [19] N. Mokari, K. Navaie, and M. Khoshkholgh, "Downlink radio resource allocation in OFDMA spectrum sharing environment with partial channel state information," *IEEE Trans. Wireless Commun.*, vol. 10, no. 10, pp. 3482–3495, Oct. 2011.
- [20] D. Xu, E. Jung, and X. Liu, "Optimal bandwidth selection in multi-channel cognitive radio networks: How much is too much?" in *Proc. 3rd IEEE Symp. New Frontiers Dyn. Spectr. Access Netw.*, Oct. 2008, pp. 1–11.
- [21] (2012). *IEEE 802.22 WRAN WG*. Accessed on: Oct. 2013. [Online]. Available: <http://www.ieee802.org/22/>
- [22] W. Zhang, C. K. Yeo, and Y. Li, "A MAC sensing protocol design for data transmission with more protection to primary users," *IEEE Trans. Mobile Comput.*, vol. 12, no. 4, pp. 621–632, Apr. 2013.
- [23] S. P. Boyd and L. Vandenberghe, *Convex Optimization*. Cambridge, U.K.: Cambridge Univ. Press, 2004.
- [24] D. P. Palomar and M. Chiang, "A tutorial on decomposition methods for network utility maximization," *IEEE J. Sel. Areas Commun.*, vol. 24, no. 8, pp. 1439–1451, Aug. 2006.
- [25] A. Charnes and W. W. Cooper, "Programming with linear fractional functionals," *Naval Res. Logistics Quart.*, vol. 9, nos. 3–4, pp. 181–186, 1962.
- [26] L. Wang, M. Sheng, X. Wang, Y. Zhang, and X. Ma, "Mean energy efficiency maximization in cognitive radio channels with PU outage constraint," *IEEE Commun. Lett.*, vol. 19, no. 2, pp. 287–290, Feb. 2015.
- [27] W. Dinkelbach, "On nonlinear fractional programming," *Manage. Sci.*, vol. 13, no. 7, pp. 492–498, Mar. 1967. [Online]. Available: <http://www.jstor.org/stable/2627691>
- [28] A. Singh, M. R. Bhatnagar, and R. K. Mallik, "Cooperative spectrum sensing in multiple antenna based cognitive radio network using an improved energy detector," *IEEE Commun. Lett.*, vol. 16, no. 1, pp. 64–67, Jan. 2012.
- [29] Y. Wang, P. Ren, F. Gao, and Z. Su, "A hybrid underlay/overlay transmission mode for cognitive radio networks with statistical quality-of-service provisioning," *IEEE Trans. Wireless Commun.*, vol. 13, no. 3, pp. 1482–1498, Mar. 2014.
- [30] J. Tang, D. K. C. So, E. Alsusa, K. A. Hamdi, A. Shojaeifard, and K. K. Wong, "Energy-efficient heterogeneous cellular networks with spectrum underlay and overlay access," *IEEE Trans. Veh. Technol.*, vol. 67, no. 3, pp. 2439–2453, Mar. 2018.
- [31] H. Hu, H. Zhang, and Y. C. Liang, "On the spectrum- and energy-efficiency tradeoff in cognitive radio networks," *IEEE Trans. Commun.*, vol. 64, no. 2, pp. 490–501, Feb. 2016.



**DEEPAK G. C.** received the B.E. degree in electronics engineering from Pokhara University, Nepal, the M.Sc. degree in computer engineering from Chonbuk National University, South Korea, and the Ph.D. degree from the InfoLab21 Lancaster University, U.K., in 2017. He joined Liverpool John Moores University, U.K., as a Research Associate with the European Union H2020 project Wi-5. He is currently with the School of Computer Science and Mathematics, Kingston University London, as a Research Associate. His research interest includes radio access technologies, cognitive radio, 5G, spectrum sensing, Internet-of-Things and public safety communications.



**KEIVAN NAVAIE** is currently with the School of Computing and Communications, Lancaster University, U.K. His research interests lie in the field of mobile computing, radio resource allocation, cognitive radio networks, and cooperative communications. He is on the Editorial Board of the IEEE TRANSACTION ON WIRELESS COMMUNICATIONS, the IEEE COMMUNICATIONS SURVEYS AND TUTORIALS, and the IEEE COMMUNICATIONS LETTERS. He has served on the Technical Program Committee for several IEEE conferences, including GlobeCom, ICC, VTC, and WCNC, and chaired some of their symposia. He has also served as the Chair of the Wireless Network Track, the IEEE VTC-2012 Yokohama, Japan, the IEEE 8th International Workshop on Wireless Network Measurements WiNMe 2012, Paderborn, Germany, the IEEE Wireless Networks and Security Track, the IEEE VTC2014 Spring, Seoul, South Korea, the Mobile and Wireless Networks Track, and the IEEE WCNC 2014, Istanbul, Turkey. He is an IET Fellow and a Chartered Engineer.



**QIANG NI** received the B.Sc., M.Sc., and Ph.D. degrees in engineering from the Huazhong University of Science and Technology, China. He led the Intelligent Wireless Communication Networking Group with Brunel University London, U.K. He is currently a Professor and the Head of the Communication Systems Group, InfoLab21, School of Computing and Communications, Lancaster University, Lancaster, U.K. His main research interests lie in the areas of wireless communications and networking, including green communications, cognitive radio systems, 5G, Internet-of-Things, and vehicular networks. He was an IEEE 802.11 Wireless Standard Working Group Voting Member and a Contributor to the IEEE Wireless Standards.

...